

# Quantum entanglement at the $\psi(3770)$ and $\Upsilon(4S)$

B.D. Yabsley

School of Physics, University of Sydney, NSW 2006, Australia.

We review results which explicitly depend on the entanglement of neutral meson pairs produced at the  $\psi(3770)$  and  $\Upsilon(4S)$ . Time-dependent CP-violation analyses at the B-factories use the flavour-singlet final state at the  $\Upsilon(4S)$ , but by assuming its quantum-mechanical evolution; Belle on the other hand has tested the time-dependent flavour correlation of the B-mesons, comparing predictions of quantum mechanics, spontaneous disentanglement, and Pompili-Selleri models. At the  $\psi(3770)$ , decay rates are modulated by various combinations of the charm mixing parameters: this has been exploited by CLEO-c to provide the first effective constraint on the strong-phase difference  $\delta$ . Finally, the goal of a “model-independent”  $\phi_3$ /Dalitz analysis is now within reach, using D-mesons from the  $\psi(3770)$  to constrain the  $D^0 \rightarrow K_S^0 \pi^+ \pi^-$  decay amplitude. Manifestly entangled events  $\psi(3770) \rightarrow (K_S^0 \pi^+ \pi^-)_D (K_S^0 \pi^+ \pi^-)_D$ , rather than just “CP-tagged” decays, turn out to be crucial.

## 1. Introduction

Einstein-Podolsky-Rosen correlations [1], in the form cited by Bohm [2], are one of the most celebrated features of quantum mechanics. For a spin-singlet state of photons or particles,

$$\frac{1}{\sqrt{2}} [|\uparrow\uparrow\rangle_1 |\downarrow\downarrow\rangle_2 - |\downarrow\downarrow\rangle_1 |\uparrow\uparrow\rangle_2], \quad (1)$$

measurements on particle 1 (2) are indeterminate, but once made they fully determine the result of a measurement on particle 2 (1). For the arrangement shown in Fig. 1, Bell’s theorem [3] (in the CHSH [4] form) shows that

$$|S| \equiv \left| E(\vec{a}, \vec{b}) - E(\vec{a}, \vec{b}') + E(\vec{a}', \vec{b}) + E(\vec{a}', \vec{b}') \right| \leq 2 \quad (2)$$

for any local realistic model; quantum mechanics allows for  $|S|$  as large as  $2\sqrt{2}$  for an optimal choice of settings.<sup>1</sup> Results breaching the bound (2) thus rule out local realism, even if we subsequently “get behind” quantum mechanics to a more complete theory: the quantum weirdness, or at least this part of it, is a phenomenon of nature.

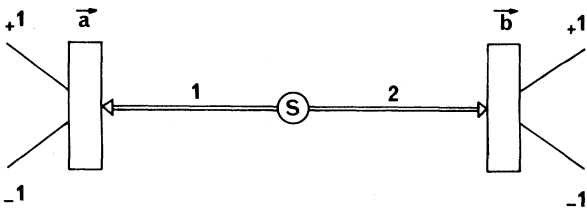


Figure 1: Bohm’s version of the EPR “experiment”. From [5].

<sup>1</sup>Here  $E$  is the correlation of measurements  

$$E(\vec{a}, \vec{b}) = \frac{R_{++}(\vec{a}, \vec{b}) + R_{--}(\vec{a}, \vec{b}) - R_{+-}(\vec{a}, \vec{b}) - R_{-+}(\vec{a}, \vec{b})}{R_{++}(\vec{a}, \vec{b}) + R_{--}(\vec{a}, \vec{b}) + R_{+-}(\vec{a}, \vec{b}) + R_{-+}(\vec{a}, \vec{b})}$$

As shown by Aspect *et al.* [5], and many times since, the bound (2) is broken for photons produced in cascade decays, with correlated polarizations: the data moreover are consistent with quantum mechanics. (The Aspect result was  $S = 2.697 \pm 0.015$ , *cf.*  $S_{QM} = 2.70 \pm 0.05$ .)

This behaviour is less well-tested for massive systems, but is nonetheless routinely used. Decay of a vector meson to a pair of neutral pseudoscalars,

$$e^+ e^- \rightarrow \Upsilon(4S) \rightarrow \frac{1}{\sqrt{2}} (|B^0\rangle |\bar{B}^0\rangle - |\bar{B}^0\rangle |B^0\rangle), \quad (3)$$

produces a B-pair entangled in a *flavour* singlet state: the flavours of the individual B-mesons are indeterminate, but at a given time  $t$ , the pair is always  $B^0 \bar{B}^0$ . In the flagship measurements of time-dependent CP violation at the B-factories, one B-meson  $B_{TAG}^0$  is reconstructed in a state of definite flavor, and the other  $B_{CP}^0$  in an eigenstate of CP. The decay rate is then modulated in the difference of decay times  $\Delta t \equiv t_1 - t_2$ ,

$$\Gamma_{CP}(\Delta t) = \frac{e^{-|\Delta t|/\tau_{B^0}}}{4\tau_{B^0}} [1 \pm \{S_{CP} \sin(\Delta m \Delta t) + A_{CP} \cos(\Delta m \Delta t)\}], \quad (4)$$

with one rate for  $B_{TAG}^0$  (+) and another rate for  $\bar{B}_{TAG}^0$  (-). The coefficients  $S_{CP}$  and  $A_{CP}$  in (4) are thus CP-violating.

A complementary measurement, assuming the B-physics but testing the time-dependent flavour oscillation due to the entanglement (3), has been performed by Belle (Section 2). In the formally equivalent, but experimentally different setting of  $\psi(3770)$  decays, decay rates of D-meson pairs are modulated by the charm mixing parameters ( $x, y$ ) and the strong phase difference  $\delta$ : CLEO-c has exploited this to derive a constraint on the latter quantity (Section 3). The final state  $\psi(3770) \rightarrow (K_S^0 \pi^+ \pi^-)_D (K_S^0 \pi^+ \pi^-)_D$ , where the entanglement of the D-mesons is clearly manifest, also turns out to be crucial for the “model-independent” measurement of the unitarity angle  $\phi_3$  using the Dalitz analysis method at the B-factories (Section 4).

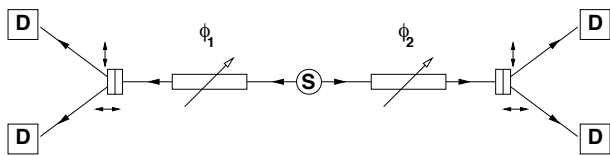


Figure 2: An optical analogue of the  $\Upsilon(4S) \rightarrow B\bar{B}$  EPR correlation analysis.

## 2. $\Upsilon(4S)$ : EPR correlations at Belle

In the *quasi-spin* analogy initially expounded for K-mesons [6], a  $|B^0\rangle$  corresponds to a spin  $|\uparrow\rangle_z$  particle or a photon with vertical polarization (V); a  $|\bar{B}^0\rangle$  corresponds to a spin  $|\downarrow\rangle_z$  particle or a horizontally polarized photon (H). While optical measurements can be made on arbitrary axes  $\alpha|\uparrow\rangle + \beta|\downarrow\rangle$ , only the  $|\uparrow\rangle$  and  $|\downarrow\rangle$  measurements are practical for B-mesons. However, over time  $t$  the state  $|B^0\rangle$  evolves to

$$\frac{1}{2} [\{1 + \cos(\Delta m_d t)\}|B^0\rangle + \{1 - \cos(\Delta m_d t)\}|\bar{B}^0\rangle], \quad (5)$$

making other “measurement axes” accessible. Thus for B-pairs produced in the flavour singlet state (3), the *decay time difference*  $\Delta m_d \Delta t$  plays the role of the difference  $\Delta\phi$  between polarimeter orientations in an optical experiment. An optical analogue of the situation at the B-factories is shown in Fig. 2: the polarimeters are fixed such that they always perform a V/H measurement on the photons, but phase rotations  $\phi_1$  and  $\phi_2$  are inserted between the production point of the entangled photons and their measurement.

This setup would seem to allow a full Bell inequality test, but in fact the rotations  $\phi_{1,2}$  are imposed by nature—in the decay times of the particles—rather than being subject to the experimenter’s choice. Thus a true Bell test cannot be performed.

### 2.1. The Green Baize Table Conspiracy Model

While there are general arguments for the impossibility of such a test [7],<sup>2</sup> it is more entertaining to consider counter-examples. A breathtakingly *unrealistic* local-realistic model, indistinguishable in its predictions from quantum mechanics, was devised for this purpose by Bramon, Escribano, and Garbarino [8]

<sup>2</sup>It turns out that even in the case of active flavor measurement (rather than letting the mesons decay), a Bell inequality test cannot be performed, because the decay of the B-mesons is too rapid compared to their flavour oscillation, *i.e.*  $x_d = \Delta m_d / \Gamma_d \simeq 0.77$  is too small.



Figure 3: According to one local-hidden-variable model, the Cigarette-Smoking Man takes a close interest in  $\Upsilon(4S) \rightarrow B\bar{B}$  decays.

(following Kasday [9]): we expound it here in a form inspired by one of the myths of our age.

Somewhere, there is a wood-panelled room with a green baize table, where powerful men meet together, smoke, and make conspiracy (Fig. 3). They determine world events in detail, including decays  $\Upsilon(4S) \rightarrow B\bar{B}$ . At the time of each decay,  $t = 0$ , four hidden variables are set: mesons 1 and 2 are each given a piece of paper (as it were) bearing the quantities  $(t_1, f_1)$  and  $(t_2, f_2)$ . These act locally: meson  $i$  decays at a time  $t = t_i$ , into final state  $f = f_i$ , according to the values written on its piece of paper. Now as part of the conspiracy, in order to deceive the world,  $(t_1, f_1, t_2, f_2)$  are chosen randomly according to quantum mechanical rules.

The phenomena in this model are indistinguishable from those in quantum mechanics, even though the individual particles have a definite state at all times: the model is local, and (if only in this sense) realistic.<sup>3</sup> Another explicit counter-example has since been constructed by Santos [11].

### 2.2. QM versus specific LR models

The best that can be done is thus to test the data in detail against quantum mechanics, and the predictions of specific local realistic models. Reasonable, non-conspiratorial models can then potentially be ruled out. The experimental quantity of choice is the time-dependent asymmetry of decay rates to opposite-flavour (OF) and same-flavour (SF) final

<sup>3</sup>Optical experiments do not share this vulnerability. For example, in the modification of the Aspect experiment reported by Weihs *et al.* [10], the effective polarimeter orientation is changed while the photons are in flight, according to randomly generated numbers. In this case, no conspiracy can fix the results to conform to a particular pattern in  $\Delta\phi \equiv \Delta m_d \Delta t$ .

states:

$$A(t_1, t_2) \equiv \frac{R_{OF}(t_1, t_2) - R_{SF}(t_1, t_2)}{R_{OF}(t_1, t_2) + R_{SF}(t_1, t_2)} \quad (6)$$

$$= \cos(\Delta m_d \Delta t) \quad (7)$$

for quantum mechanics. The dependence on  $\Delta t = t_1 - t_2$  alone, a consequence of the entanglement of the state, is distinctive. It's therefore useful to consider asymmetries as functions not of  $(t_1, t_2)$ , but of  $\Delta t$  and  $t_{\min} \equiv \min(t_1, t_2)$ . Several possibilities for  $A(\Delta t, t_{\min})$  are shown in Fig. 4. As a limiting case, under spontaneous disentanglement (SD) to a  $B^0\bar{B}^0$  pair (with definite flavour) immediately after  $\Upsilon(4S)$  decay, the two mesons undergo independent flavor oscillations, with

$$A_{SD} = \cos(\Delta m_d t_1) \cos(\Delta m_d t_2), \quad (8)$$

taking the complicated form in the figure when plotted on  $(\Delta t, t_{\min})$ . More seriously, one can consider the class of models obeying the assumptions of Pompili and Selleri [12]: QM-like states for the individual mesons with stable mass; 100% flavour correlations, to reproduce the QM behaviour as closely as possible; and the constraint that QM predictions for uncorrelated B-mesons should also be preserved. Asymmetries must then lie between the bounds

$$\begin{aligned} A_{PS}^{\min} &= 1 - \min(2 + \Psi, 2 - \Psi), \text{ where} \\ \Psi &= \{1 + \cos(\Delta m_d \Delta t)\} \cos(\Delta m_d t_{\min}) \\ &\quad - \sin(\Delta m_d \Delta t) \sin(\Delta m_d t_{\min}) \end{aligned} \quad (9)$$

and

$$\begin{aligned} A_{PS}^{\max} &= 1 - |\{1 - \cos(\Delta m_d \Delta t)\} \cos(\Delta m_d t_{\min}) \\ &\quad + \sin(\Delta m_d \Delta t) \sin(\Delta m_d t_{\min})| \end{aligned} \quad (10)$$

shown in the figure.

In the current state of the art, the discrimination power shown in Fig. 4 is not fully realised, as only  $\Delta t$  is measured: the expressions (8)–(10) must in effect be integrated over  $t_{\min}$ . It turns out that it is still possible to exclude the local-realistic models shown.

### 2.3. The 2007 Belle result

The Belle analysis [13] is based on a  $152 \times 10^6$   $B\bar{B}$  data sample, and uses techniques established for time-dependent CP-violation analyses: one B-meson is reconstructed in a flavour-tagging mode  $B^0 \rightarrow D^{*-} \ell^+ \nu$ , while the other B-flavour is tagged using a lepton; a consistency check with other flavour-tagging information is imposed to maintain purity. A sample of 8565 such events is found: 6718 opposite-flavour, and 1847 same-flavour pairs, divided into 11 bins in  $\Delta t$ .

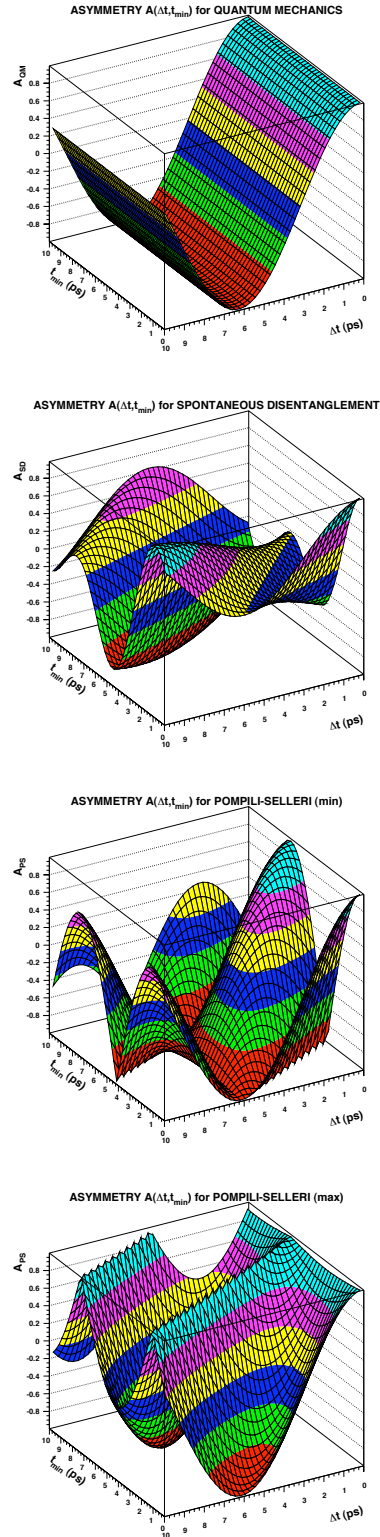


Figure 4: For ideal measurement at  $\Upsilon(4S) \rightarrow B\bar{B}$ : decay rate asymmetry  $A = (R_{OF} - R_{SF})/(R_{OF} + R_{SF})$  as a function of  $(\Delta t, t_{\min})$ , (top) for quantum mechanics; (second) for spontaneous disentanglement; and for the Pompili-Selleri class of models, showing (third) minimum, and (bottom) maximum values.

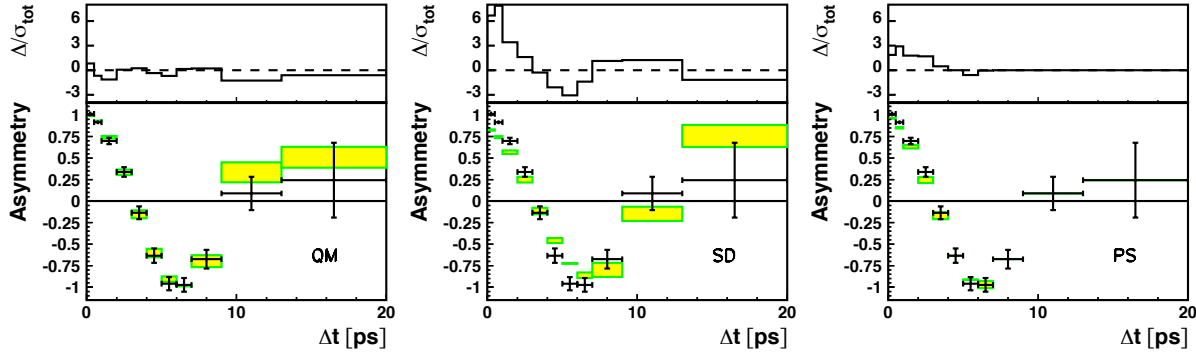


Figure 5: From [13]: Asymmetries as a function of  $\Delta t$  in Belle data, compared to (left) quantum mechanics, (middle) spontaneous disentanglement, and (right) Pompili-Selleri models. The lower plots show time-dependent flavour asymmetry (crosses) and the results of weighted least-squares fits to each model (rectangles, showing  $\pm 1\sigma$  errors on  $\Delta m_d$ ). Upper plots show differences  $\Delta \equiv A_{\text{data}} - A_{\text{model}}$  in each bin, divided by the total experimental error  $\sigma_{\text{tot}}$ . Bins where  $A_{\text{PS}}^{\text{min}} < A_{\text{data}} < A_{\text{PS}}^{\text{max}}$  have been assigned a null deviation.

Backgrounds are subtracted from the OF and SF samples separately, in  $\Delta t$  bins: fake  $D^*$ , using sidebands ( $126 \pm 6$  OF,  $54 \pm 4$  SF); bad  $D^* - \ell$  combinations, also from data ( $78 \pm 9$  OF,  $236 \pm 15$  SF); and  $B^+ \rightarrow \bar{D}^{*0} \ell \nu$  events, estimated from Monte Carlo and the  $\cos_{B,D^* \ell}$  distribution in data (254 OF and 1.5 SF [both  $\pm 6\%$ ]). This process is crucial, as the backgrounds produce a time-structured difference in the asymmetry. After a  $(1.5 \pm 0.5)\%$  correction for mistagging, deconvolution is performed (using DSVD, on the SF and OF samples separately) to remove decay-vertex-resolution, efficiency, and other remaining effects. (Potential bias against any of the models is explicitly studied and subtracted, with a systematic error assigned.) Finally, a simple exponential fit to the resulting histogram is performed, to extract the B-lifetime as a check:  $\tau_{B^0} = (1.532 \pm 0.017)$  ps is found, *cf.* the  $(1.530 \pm 0.009)$  ps world average [14].

A comparison between the data, and fits to the predictions of each model, is shown in Fig. 5. In each case, the parameter  $\Delta m_d$  is floated, subject to the constraint of the world average value, with Belle and BaBar contributions excluded:  $(0.496 \pm 0.014)$  ps $^{-1}$  [15].<sup>4</sup> Quantum mechanical predictions fit the data well ( $\chi^2/n_{\text{dof}} = 5/11$ ), while spontaneous disentanglement is disfavoured at  $13\sigma$  ( $\chi^2 = 174$ ). A fit to  $(1 - \zeta_{B^0 \bar{B}^0}) A_{\text{QM}}(\Delta t) + \zeta_{B^0 \bar{B}^0} A_{\text{SD}}(\Delta t)$  finds an “SD fraction” of  $\zeta_{B^0 \bar{B}^0} = 0.029 \pm 0.057$ , consistent with zero.<sup>5</sup> The entire class of local realistic models satisfying the minimal Pompili-Selleri assumptions is disfavoured at  $5.1\sigma$  ( $\chi^2 = 31$ ).

<sup>4</sup>The Belle and BaBar results are from fits assuming QM time evolution, and so cannot be used. They otherwise dominate the average, improving its precision by a factor of three.

<sup>5</sup>In a decoherence model, this is equivalent to multiplying the interference term in the  $B^0 - \bar{B}^0$  basis by a factor  $(1 - \zeta_{B^0 \bar{B}^0})$  [16].

### 3. $\psi(3770)$ : $(x, y, \delta)$ and rates at CLEO-c

Formally, the situation at the  $\psi(3770)$  is the same as that at the  $\Upsilon(4S)$ : the decay  $e^+e^- \rightarrow \psi(3770) \rightarrow \frac{1}{\sqrt{2}}(|D^0\rangle|\bar{D}^0\rangle - |\bar{D}^0\rangle|D^0\rangle)$  leads to an entangled final state equivalent to (3). However there are differences in practice: mixing is a percent-level effect in D-decay amplitudes, and CP violation is suppressed orders of magnitude further. So while the principal use of the state (3) at the  $\Upsilon(4S)$  is study of CP violation, an obvious use of D-meson pairs produced at the  $\psi(3770)$  is CP tagging. For example, decays to two CP-even (or two CP-odd) eigenstates don’t occur.

If we consider decays  $\psi(3770) \rightarrow (K^- \pi^+)_D (K^- \pi^+)_D$ , however, the situation is not so straightforward. Relative to production from a pair of  $D^0$  mesons, the rate is suppressed by the mixing rate  $R_M = \frac{1}{2}(x^2 + y^2)$ ; by contrast, the rate for uncorrelated  $D\bar{D}$  decays to this final state is suppressed by only the “wrong-sign” rate  $R_{WS}$ , *i.e.* it is forty times larger. There are thus nontrivial effects due to the coherence of the state produced at the  $\psi(3770)$ . Currently the most systematic treatment is [17], following earlier work by [18] and others.

#### 3.1. $D^0 \rightarrow K_{S,L}^0 \pi^0$

A simple example is the study of  $D^0 \rightarrow K_L^0 \pi^0$  by CLEO-c [19], where the  $D^0 \rightarrow K_L^0 \pi^0$  decay is recovered using the distribution of missing-mass-squared  $M_{\text{miss}}^2$  in events tagged by a fully-reconstructed  $\bar{D}^0$  decay. In practice there are three distinct samples, corresponding to the three tagging modes  $\bar{D}^0 \rightarrow K^+ \pi^-$ ,  $K^+ \pi^- \pi^0$ , and  $K^+ \pi^- \pi^- \pi^+$ . A  $D^0 \rightarrow K_L^0 \pi^0$  branching fraction calculation using tagging mode  $f$  in fact determines

$$\mathcal{B}_{K_L^0 \pi^0} \left( 1 + \frac{2r_f \cos \delta_f + y}{1 + R_{WS,f}} \right),$$

Table I From [20]. Effective branching fractions (upper section) for  $D^0$  decay modes  $i$ , divided by  $\mathcal{B}_i$ , and (lower section) for  $D^0\bar{D}^0$  decay to modes  $\{i, j\}$ , divided by  $\mathcal{B}_i\mathcal{B}_j$ , in  $\psi(3770) \rightarrow \frac{1}{\sqrt{2}}(|D^0\rangle|\bar{D}^0\rangle - |\bar{D}^0\rangle|D^0\rangle)$  data.  $S_+$  ( $S_-$ ) denotes a CP-even (CP-odd) eigenstate, and  $e^-$  a semileptonic final state  $X^+e^-\bar{\nu}_e$ . Quantities are shown to leading order in the mixing parameters  $(x, y)$  and the wrong-sign rate  $R_{WS}$ .  $R_M = \frac{1}{2}(x^2 + y^2)$  is the mixing rate.

Mode	Correlated	Uncorrelated
$K^-\pi^+$	$1 + R_{WS}$	$1 + R_{WS}$
$S_+$	2	2
$S_-$	2	2
$K^-\pi^+, K^-\pi^+$	$R_M$	$R_{WS}$
$K^-\pi^+, K^+\pi^-$	$[(1 + R_{WS})^2 - 4r \cos \delta (r \cos \delta + y)]$	$1 + R_{WS}^2$
$K^-\pi^+, S_+$	$1 + R_{WS} + 2r \cos \delta + y$	$1 + R_{WS}$
$K^-\pi^+, S_-$	$1 + R_{WS} - 2r \cos \delta - y$	$1 + R_{WS}$
$K^-\pi^+, e^-$	$1 - ry \cos \delta - rx \sin \delta$	1
$S_+, S_+$	0	1
$S_-, S_-$	0	1
$S_+, S_-$	4	2
$S_+, e^-$	$1 + y$	1
$S_-, e^-$	$1 - y$	1

where the amplitude ratio  $r_f$  and strong phase difference  $\delta_f$  ( $r_f e^{-i\delta_f} \equiv \langle f|\bar{D}^0\rangle/\langle f|D^0\rangle$ ) and the wrong-sign rate  $R_{WS,f}$  are mode-dependent.

The method is to use the equivalent measurement for  $D^0 \rightarrow K_S^0\pi^0$ , an untagged measurement of the branching fraction for that mode, to determine the product  $C_f = (2r_f \cos \delta_f + y)/(1 + R_{WS,f})$ . (A tagged analysis in this mode finds an effective branching fraction  $\mathcal{B}_{K_S^0\pi^0}(1 - C_f)$ .) The true  $D^0 \rightarrow K^0\pi^0$  branching fraction can then be measured for each tagged sample: averaging over them, CLEO-c find

$$\mathcal{B}_{K_L^0\pi^0} = (0.998 \pm 0.049 \pm 0.030 \pm 0.038)\%, \quad (11)$$

and an asymmetry

$$\frac{\mathcal{B}_{K_S^0\pi^0} - \mathcal{B}_{K_L^0\pi^0}}{\mathcal{B}_{K_S^0\pi^0} + \mathcal{B}_{K_L^0\pi^0}} = 0.108 \pm 0.025 \pm 0.024, \quad (12)$$

consistent with the value  $2 \tan \theta_C = 0.109 \pm 0.001$  expected if symmetry under the U-spin subgroup of SU(3) is imposed.

### 3.2. Charm mixing and $\delta$

In the general case, effective branching fractions depend on the mixing parameters  $(x, y)$ , and (for the  $K^-\pi^+$  final state) the strong phase difference  $\delta \equiv \delta_{K\pi}$ . Correction factors are summarized in Table I. Whereas in the  $D^0 \rightarrow K_L^0\pi^0$  analysis the corrections were a complication that needed to be taken into

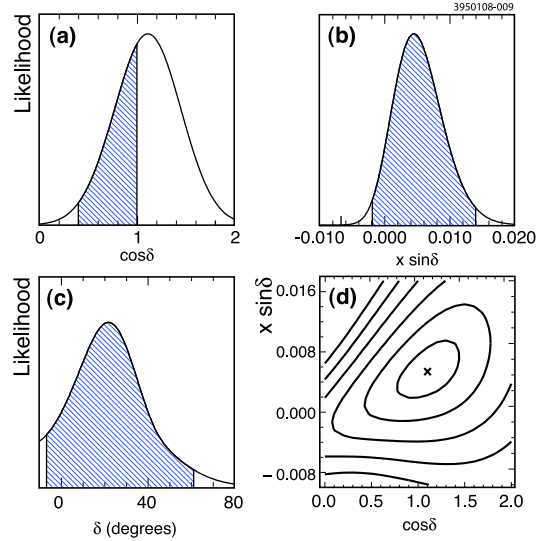


Figure 6: From [20]: Constraints on the strong phase difference  $\delta$ , after combining results from CLEO-c's entangled source of D-mesons with external branching fraction and mixing parameter measurements. Likelihood curves (including statistical and systematic uncertainties) are shown for (a)  $\cos \delta$ , (b)  $x \sin \delta$ , and (c)  $\delta$ ; (d) shows contours in units of  $\sqrt{\Delta\chi^2}$  on  $(\cos \delta, x \sin \delta)$ .

account, the CLEO-c analysis reported in [20] uses a suite of measurements, and their varying dependence on  $(x, y)$  and  $\delta$ , to constrain the mixing parameters, and in particular  $\delta$ .

In the first case a least-squares fit is performed to the yields in eight hadronic final states ( $K^-\pi^+$ ,  $K^+\pi^-$ ,  $K^+K^-$ ,  $\pi^+\pi^-$ ,  $K_S^0\pi^0\pi^0$ ,  $K_S^0\pi^0$ ,  $K_S^0\eta$ , and  $K_S^0\omega$ ), and 43 “double-tagged” final states (24 fully-reconstructed, 14 including a semileptonic decay, and 5 including  $K_L^0\pi^0$ ), together with external results on seven branching fractions (CP eigenstates, and  $K^-\pi^+$ , with correlations taken into account). The result finds the lifetime difference parameter  $y$  with large uncertainty, and as a result the combination  $x \sin \delta$  is unconstrained.

An extended fit, including measurements of mixing-related quantities ( $y, x, r^2, y', (x')^2$ ) by other experiments, is therefore performed: results are shown in Fig. 6. The fit finds

$$\begin{aligned} \cos \delta &= 1.10 \pm 0.35 \pm 0.07 \\ x \sin \delta &= (4.4_{-1.8}^{+2.7} \pm 2.9) \times 10^{-3}, \end{aligned} \quad (13)$$

and after minimising on the physical surface  $(\cos \delta, \sin \delta)$ ,

$$\begin{aligned} \delta &= (22_{-12}^{+11+9})^\circ, \text{ with} \\ \delta &\in [-7^\circ, +61^\circ] \text{ at 95\% confidence,} \end{aligned} \quad (14)$$

the first effective constraint on this quantity. Together with the external mixing measurements (without which the analysis is not possible), the precision

on  $\cos \delta$  is driven by the yields for the eight hadronic final states, and double-tag yields  $\{K\pi, S_{\pm}\}$  including CP-eigenstates  $S_{\pm}$ . These results are for a  $281 \text{ pb}^{-1}$  sample: better precision will be possible with the final CLEO-c dataset.

#### 4. $\phi_3/\text{Dalitz}$ : $\psi(3770)$ rescues the $\Upsilon(4S)$

Dalitz analyses of  $B^{\pm} \rightarrow DK^{\pm}$  and  $D^*K^{\pm}$ , with  $D \rightarrow K_S^0\pi^+\pi^-$  and  $K_S^0K^+K^-$ , are currently the most sensitive probe of the unitarity angle  $\phi_3$  (also known, in the least interesting of the disagreements between the B-factories, as  $\gamma$ ). The state of play in these important analyses was shown in Anton Poluektov's talk on Monday [21]; Belle's preliminary update [22], shown in Fig. 7, finds  $\phi_3 = (76_{-13}^{+12} \pm 4 \pm 9)^{\circ}$ ; BaBar's new publication [23], shown in Fig. 8, finds  $\phi_3 = (76 \pm 22 \pm 5 \pm 5)^{\circ}$ . In both cases, the model error (shown last) is already uncomfortably large.

The future of this measurement is the so-called model-independent approach [24]; the feasibility study for the method has recently been updated [25]. Rather than relying directly on (say) an isobar model to determine the  $\bar{D}^0 \rightarrow K_S^0\pi^+\pi^-$  decay amplitude, the phase difference parameters

$$\begin{aligned} c &= \cos(\delta_D(m_+^2, m_-^2) - \delta_D(m_-^2, m_+^2)) \\ s &= \sin(\delta_D(m_+^2, m_-^2) - \delta_D(m_-^2, m_+^2)) \end{aligned} \quad (15)$$

are extracted from  $\psi(3770)$  data, exploiting the correlations in the final state to measure the Dalitz plot, not for  $D^0$  or  $\bar{D}^0$ , but for CP-tagged D-mesons. The challenge is to cope effectively with the limited data samples available (or foreseen).

An advance has been the nontrivial binning shown in Fig. 9, which is uniform in  $\Delta\delta_D|_{\text{model}}$ . However, results prove to be biased for finite  $D_{CP} \rightarrow K_S^0\pi^+\pi^-$  sample sizes: tests where events are generated in one model, and reconstructed using another, find a return of model dependence, as shown in Fig. 10. It arises because for each bin, of the parameters in (15), only  $c_i$  is reconstructed;  $s_i$  is recovered by a  $c_i^2 + s_i^2 = 1$  constraint. A change of model results in a shift of the  $\delta_D$  region sampled by a given bin, introducing a bias in  $s_i$  via the constraint.

The study [25] finds that if  $\{c_i, s_i\}$  are determined from  $\psi(3770) \rightarrow (K_S^0\pi\pi)_D(K_S^0\pi\pi)_D$  events, the outcome is unbiased for finite data samples: a change of model can degrade the sensitivity (Fig. 10), but not introduce a bias. The importance of the entangled final state at the  $\psi(3770)$  thus goes beyond ‘‘CP-tagging’’: the additional correlations in the final state  $(K_S^0\pi\pi)_D(K_S^0\pi\pi)_D$  are crucial.

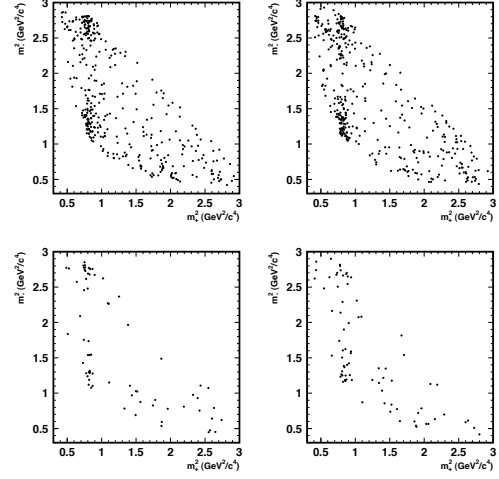


Figure 7: From [22]: (preliminary) updated Belle results. Dalitz distributions for  $\bar{D}^0 \rightarrow K_S^0\pi^+\pi^-$  decays from (top)  $B^{\pm} \rightarrow DK^{\pm}$  and (bottom)  $B^{\pm} \rightarrow D^*K^{\pm}$ , for (left)  $B^+$  and (right)  $B^-$  samples.

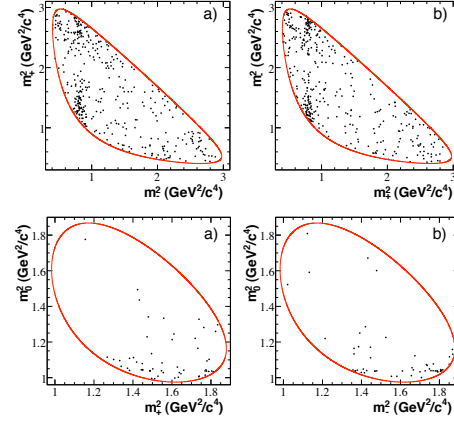


Figure 8: From [23]: a selection of (published) BaBar results. Dalitz distributions of (Upper)  $\bar{D}^0 \rightarrow K_S^0\pi^+\pi^-$  for (a)  $B^- \rightarrow DK^-$  and (b)  $B^+ \rightarrow DK^+$ ; and (lower)  $\bar{D}^0 \rightarrow K_S^0K^+K^-$  for (a)  $B^- \rightarrow DK^-$  and (b)  $B^+ \rightarrow DK^+$ .

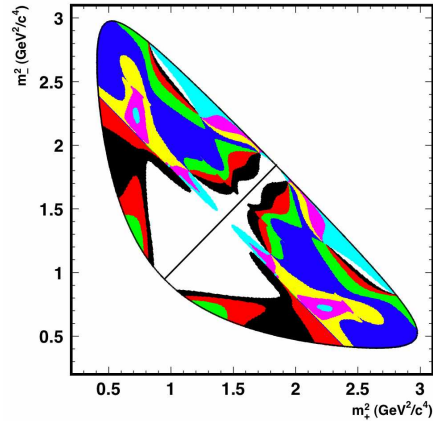


Figure 9: From [25]: Uniform binning in  $\Delta\delta_D|_{\text{model}}$  on the  $\bar{D}^0 \rightarrow K_S^0\pi^+\pi^-$  Dalitz plot; see the text.

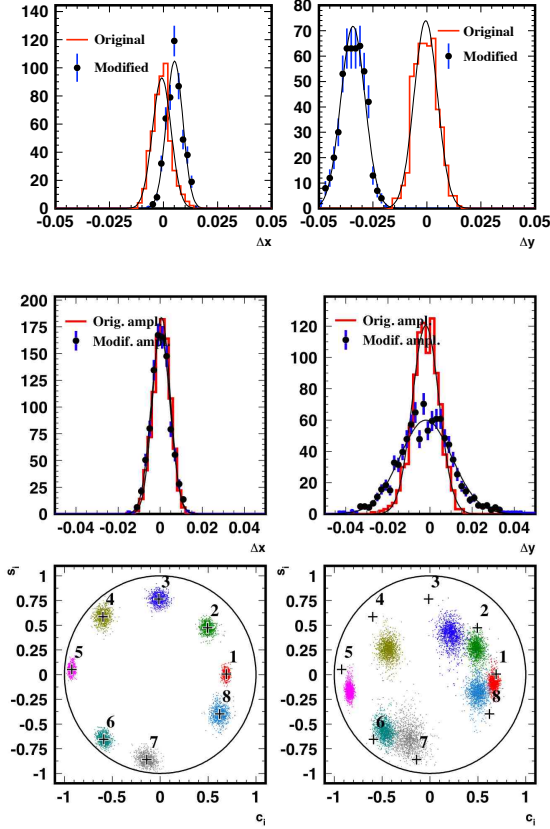


Figure 10: From [25], showing results of toy Monte Carlo simulation of the  $\phi_3$ /Dalitz analysis. (Top:) using  $D_{CP}$  data; the histogram shows fit results where the same  $D^0$  decay amplitude is used for generation and binning, and the points with error bars show the case with different amplitudes. (Middle:) as above, but using  $\psi(3770) \rightarrow (K_S^0 \pi^+ \pi^-)_D (K_S^0 \pi^+ \pi^-)_D$  data. (Bottom:) coefficients  $(c_i, s_i)$  obtained from the eight  $\Delta\delta_D|_{model}$  bins of Fig. 9, where (left) the same amplitude, and (right) different amplitudes are used for event generation and binning.

## 5. Summary

Analyses which explicitly depend on the entanglement of neutral meson pairs are becoming important in this field. The effect allows the model-dependence in  $\phi_3$ /Dalitz analyses to be lifted: CLEO-c data will already be necessary to enable full use to be made of final B-factory results; BESIII results will be needed to exploit the data from a super-B/ﬂavor factory. Entanglement in  $\psi(3770) \rightarrow D^0 \bar{D}^0$  modulates tagged decay rates in a way that must be taken into account for  $D^0 \rightarrow K_L^0 \pi^0$  measurement, and that has now enabled the first effective constraint,  $\delta_{K\pi} = (22^{+11+9}_{-12-11})^\circ$ , on the strong phase difference in  $D^0 \rightarrow K^+ \pi^-$ . And at the  $\Upsilon(4S)$ , entanglement, used routinely in B-factory measurements, has now been tested, even though a Bell inequality analysis cannot be performed. A constraint on the decoherent fraction  $\zeta_{B^0 \bar{B}^0} = 0.029 \pm$

0.057 is found; as for “realistic” local-realistic models, the class obeying the Pompili-Selleri assumptions has been ruled out at  $5.1\sigma$ , the first such constraint from data.

## 6. Acknowledgements

As well as expressing my appreciation to the FPCP 2008 conference organisers, I must thank my collaborators on Belle for discussions during the preparation of the EPR correlations result: Apollo Go and Aurelio Bay (the principal authors), Nick Hastings, Mike Peters, Samo Stanič, and others. I would also like to acknowledge the contribution of colleagues at the University of Queensland. A preliminary version of the Belle results were presented at a colloquium there in late 2006, and the optical analogy in Fig. 2 was developed during stimulating discussions at that time.

## References

- [1] A. Einstein, B. Podolski and N. Rosen, *Phys. Rev.* **47**, 777–780 (1935).
- [2] D. Bohm, *Quantum Theory* (Prentice Hall, Englewood Cliffs, NJ, 1951), pp 614–622.
- [3] J. S. Bell, *Physics* **1**, 195 (1964).
- [4] J.F. Clauser, M.A. Horne, A. Shimony, and R.A. Holt, *Phys. Rev. Lett.* **23**, 880–884 (1969).
- [5] A. Aspect, P. Grangier, and G. Roger, *Phys. Rev. Lett.* **49**, 91–94 (1982).
- [6] T.D. Lee and C.S. Wu, *Ann. Rev. Nucl. Sci.* **16**, 511–590 (1966); H.J. Lipkin, *Phys. Rev.* **176**, 1715–1718 (1968). R.A. Bertlmann and B.C. Hiesmayr, *Phys. Rev. A* **63**, 062112 (2001).
- [7] R.A. Bertlmann, A. Bramon, G. Garbarino, B.C. Hiesmayr, *Phys. Lett. A* **332**, 355–360 (2004).
- [8] A. Bramon, R. Escribano, and G. Garbarino, *J. Mod. Opt.* **52**, 1681–1684 (2005).
- [9] L. Kasday, “Experimental test of quantum predictions for widely separated photons”. In *Proceedings of the International School of Physics “Enrico Fermi”, Course IL: Foundations of Quantum Mechanics* (Academic Press, New York, 1971), p195.
- [10] G. Weihs, T. Jennewein, C. Simon, H. Weinfurter, and A. Zeilinger, *Phys. Rev. Lett.* **81**, 5039–5043 (1998).
- [11] E. Santos, [arXiv:quant-ph/0703206](https://arxiv.org/abs/quant-ph/0703206).
- [12] A. Pompili and F. Selleri, *Eur. Phys. J. C* **14**, 469–478 (2000).
- [13] A. Go, A. Bay *et al.* (Belle Collaboration), *Phys. Rev. Lett.* **99**, 131802 (2007).
- [14] W.-M. Yao *et al.* (Particle Data Group), *J. Phys. G* **33**, 1–1232 (2006).

- [15] E. Barberio *et al.* (Heavy Flavour Averaging Group), [arXiv:hep-ex/0603003](#).
- [16] R.A. Bertlmann, W. Grimus, and B.C. Hiesmayr, *Phys. Rev. D* **60**, 114032 (1999).
- [17] D.M. Asner and W.M. Sun, *Phys. Rev. D* **73**, 034024 (2006); **77**, 019902(E) (2008).
- [18] M. Gronau, Y. Grossman, and J.L. Rosner, *Phys. Lett. B* **508**, 37–43, (2001).
- [19] Q. He *et al.* (CLEO Collaboration), *Phys. Rev. Lett.* **100**, 091801 (2008).
- [20] J.L. Rosner *et al.* (CLEO Collaboration), *Phys. Rev. Lett.* **100**, 221801 (2008); D.M. Asner *et al.* (CLEO Collaboration), *Phys. Rev. D* **78**, 012001 (2008).
- [21] A. Poluektov, “Measurements of  $\gamma/\phi_3$  at B factories”, in these Proceedings; [arXiv:0807.1772 \[hep-ex\]](#).
- [22] I. Adachi *et al.* (Belle Collaboration), BELLE-CONF-0801; [arXiv:0803.3375 \[hep-ex\]](#).
- [23] B. Aubert *et al.* (BaBar Collaboration), *Phys. Rev. D* **78**, 034023 (2008).
- [24] A. Bondar and A. Poluektov, *Eur. Phys. J. C* **47**, 347 (2006).
- [25] A. Bondar and A. Poluektov, *Eur. Phys. J. C* **55**, 51 (2008).